Separation of Enantiomers by Enantio-Specific Interaction of Chiral Molecules with Magnetic Substrates

Koyel Banerjee-Ghosh,[1$] Oren Ben Dor,[2$] Francesco Tassinari,[1$] Eyal Capua,[1] Shira Yochelis,[2] Amir Capua,[2] See-Hun Yang,[3] Stuart Stephen Papworth Parkin,[3,4] Soumyajit Sarkar,[5] Leeor Kronik,[5] Lech Tomasz Baczewski,[6] Ron Naaman,[1*] and Yossi Paltiel[2*]

1) Dept. of Chemical and Biological Physics, Weizmann Institute of Science, Rehovot, 76100 Israel
2) Dept. of Applied Physics, Hebrew University, Jerusalem, Israel
3) IBM Research Division, Almaden Research Center, 650 Harry Road, San Jose, California 95120, USA
4) Max Planck Institute for Microstructure Physics, Halle (Saale), D-06120, Germany
5) Department of Materials and Interfaces, Weizmann Institute of Science, Rehovot, 76100 Israel
6) Institute of Physics Polish Academy of Sciences, Al. Lotnikow 32/46, 02-668 Warszawa, Poland.

[$] The first three authors contributed equally to this work.

Abstract

Enantio-selectivity is imperative in nature and many molecules in plants and living organisms possess specific enantiomeric properties. It is commonly assumed that recognition of chirality and enantio-selection, both in nature and in artificial systems, is solely related to spatial effects, with the recognition process typically described using a "lock and key"-type model. In recent years, it has been suggested that as electrons move through or as charge is redistributed in chiral molecules, an enantio-specific electron spin orientation is preferred. Therefore, for chiral molecules the induced spin polarization may affect enantio-recognition through exchange interactions. Here, we show experimentally, that the interaction of chiral molecules with a perpendicularly magnetized magnetic substrate is enantio-specific. Thus, one enantiomer adsorbs preferentially when the magnetic dipole is pointing up, whereas the other is adsorbed faster for the opposite alignment of the magnetization direction. This allows for a generic enantiomeric separation technique. The interaction is not controlled by the magnetic field *per se*, but rather by the electron spin orientations.

The relation between magnetism and chirality was the basis for a controversy that started over a century ago between two giants of science, Pasteur and Kelvin.(1,2) Pasteur, after discovering that the chemistry of life showed a preference for molecules with a particular handedness,(3,4) tried to carry out experiments aimed at finding asymmetric physical forces that can explain the biological homochirality.(5) He attempted to induce handedness by stirring the reactants in a centrifuge and by applying a magnetic field, but both attempts failed. In 2001, Ribo et al. reported that by stirring solutions of achiral porphyrins, one can induce chiral symmetry breaking in the resulting mesophases.(6) Chiral supra-molecular organization was also induced by vortex flow (7). However, all attempts to induce chirality by magnetic field only, failed.(8) This lack of success is consistent with Lord Kelvin's conclusion that "the magnetic rotation alone has neither left-handed nor right-handed quality".(9) Moreover, de Gennes has demonstrated that even the superposition of a magnetic field and an electric field, originally suggested by Curie,(10) does not allow asymmetrical reactions.(11) He claimed, however, that if the final state is out of equilibrium, asymmetry remains possible. Here, we present a new "twist" on this long-standing issue by demonstrating an enantio-selective interaction of chiral molecules with a substrate magnetized perpendicular to its surface, which is mediated by a spin-specific interaction, but not by the magnetic field *per se*.

In recent years it has been shown that when electrons move through chiral molecules, their transport is spin-dependent, with the preferred spin-orientation determined by the handedness of the molecule and the direction of motion.(12,13) The effect, which by now is well-established,(14-18) is known as chirality-induced spin selectivity (CISS). As a corollary, it was recently shown that charge redistribution in chiral molecules is also accompanied by enantio-determined spin polarization.(19) These results led us to consider the possible interaction between chiral molecules with perpendicularly-magnetized surfaces. This interaction should be spin-sensitive by virtue of short-range magnetic-exchange interactions. Therefore, it could result in enantio-specificity through the above-mentioned relation between spin and chirality via the CISS phenomenon. If this is the case, it would facilitate the separation of a racemic mixture into its two enantiomeric components simply by allowing the mixture to interact with the magnetic substrate.

Enantio-selectivity is ubiquitous in nature and many of the molecules in plants and living organisms have specific enantiomeric properties.(20) Chiral recognition and enantiomeric selectivity are commonly assumed, both in nature and in artificial systems, to be related to a spatial effect, with the recognition process typically described by a "lock and key"-type model.(21) Accordingly, chromatography-based enantio-separation requires the chiral substrate to be adjusted so as to interact optimally with a specific enantiomer.(22) With the present spin-based approach, however, enantio-separation would be general and could be applied without any special adjustment of the substrate. Here, we show that this is indeed the case and demonstrate the efficiency of the spin-based separation for several molecules that differ in size and chirality: oligopeptides, amino acids, and double stranded DNA.

As a first examination, an L- or D-PAL, a thiolated α-helix oligopeptide, SH-CAAAAKAAAAKAAAAKAAAAKAAAAKAAAAKAAAAK (C, A, and K represent cysteine, alanine, and lysine, respectively), was exposed to a ferromagnetic (FM) Co film covered with 5 nm of Au for 2 sec (see supplementary information, SI, for details). SiO_2 nanoparticles (NPs) were attached to the adsorbed PAL to act as a marker for the monolayer adsorption density. Importantly, it is known that a thin layer of a noble metal like gold or platinum (up to about 10 nm), deposited on a ferromagnet, transfers spin very efficiently and features magnetic properties and spin accumulation.(23-25) Hence, the gold layer that prevents oxidation and ensures covalent bonding through the thiol group can be viewed as part of the FM substrate. Figures 1a,b show scanning electron microscope (SEM) images of the L-enantiomer adsorbed on FM substrate, with the latter magnetized up or down, respectively. The concentration of adsorbed particles in Fig. 1a is $\sim 4 \cdot 10^{10}$ NPs/cm^2, whereas in Fig. 1b it is $\sim 6 \cdot 10^{9}$ NPs/cm^2. Results of the complementary experiment with D-PAL are shown in Figs. 1c,d, with concentrations of $\sim 1 \cdot 10^{10}$ NPs/cm^2 and $\sim 4 \cdot 10^{10}$ NPs/cm^2 found for the up and down magnetized substrate. As a control experiment, L and D enantiomers were also adsorbed on a non-magnetic, pure gold substrate, with an external magnetic field applied either normally or anti-normally to the substrate. In this case, no enantio-selectivity was observed (see a full comparison in Fig. 1e). In addition, the adsorption efficiency in this case was found to be between that of the FM substrate with the favored and unfavored spin alignment.

Moreover, when the substrate was magnetized in-plane, no selective adsorption was observed.

The above results clearly demonstrate enantio-selectivity in the adsorption process. We note that in one magnetization direction the L-PAL adsorption rate is at least 8 times faster than that of the D-PAL, whereas in the other magnetization direction the D-PAL adsorption rate is at least 4 times faster than that of L-PAL. However, the D-PAL purification level is lower than that of L-PAL, likely explaining the asymmetry in adsorption rate ratios. Furthermore, repeat of this experiment with a longer adsorption time (2 minutes) resulted in a reduction in the enantio-selectivity of adsorption (see Figure S1 and S2 in the SI), i.e., the process exhibits significant kinetic differences.

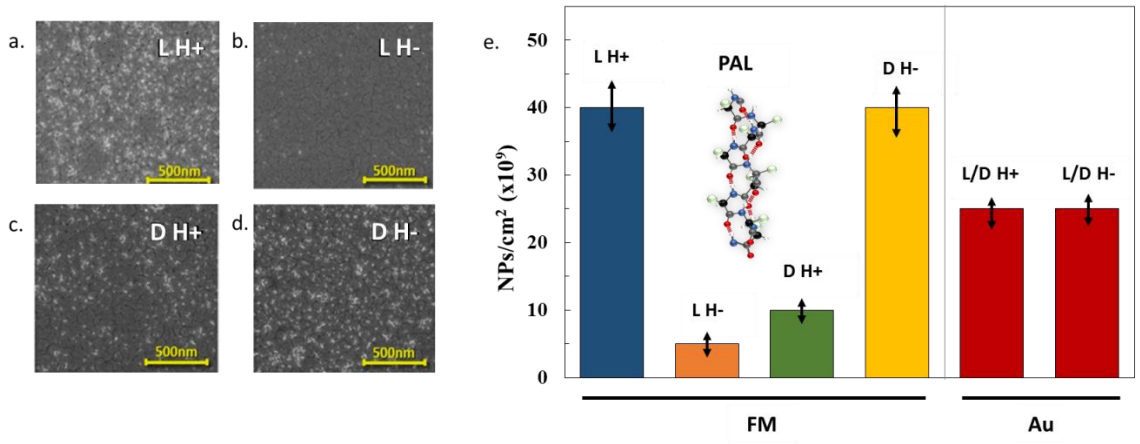

Figure 1: Adsorption of the PAL oligopeptide on ferromagnetic samples (silicon with a 1.8 nm Co film and a 5 nm Au), magnetized with the magnetic dipole pointing up (H^+) or down (H^-) relative to the substrate surface. SiO_2 nanoparticles were attached to the adsorbed oligopeptides. L-PAL (a,b) and D-PAL (c,d) were adsorbed on a substrate magnetized up or down for 2 sec. (e) Histograms summarizing the nanoparticle adsorption densities shown in (a-d), compared with the adsorption density on gold with an applied external magnetic field (in red).

So far, we demonstrated difference in the adsorption of enantio-pure molecules on a FM substrate. We now consider the separation of a racemic PAL mixture into its two enantiomeric components upon exposure to a magnetic substrate. The original mixture exhibited no circular dichroism (CD). As shown in Fig. 2a, upon multiple repeated exposures to a substrate with up or down-pointing magnetization a clear CD signature

corresponding to D and L-PAL, respectively, is obtained. Furthermore, this signature is similar to that obtained for the pure enantiomers, as shown in Figure 2b.

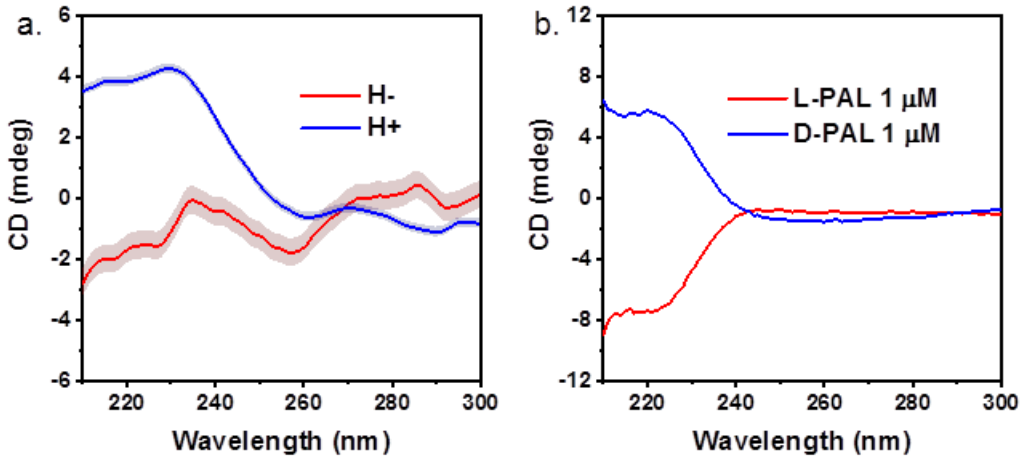

Figure 2: (a) Enantio-specific CD spectra of PAL, obtained from exposure of a racemic PAL mixture exhibiting no CD to a substrate with magnetization pointing down (red) or up (blue). CD spectra were obtained post-adsorption, with uncertainties marked by the grey-shaded area. Clearly, after the specific adsorption of one enantiomer, the resulting CD spectra indicate the presence of the opposite enantiomer. (b) CD spectra of the pure enantiomers, given for comparison.

The above arguments can be utilized to create a practical enantio-separation apparatus, based on flow through a column coated on one side with a thin (6 nm) Co/Ni layer covered by a thin (5 nm) Au layer and magnetized externally either normally or anti-normally to the surface. Figure 3 shows the CD spectra of a racemic PAL solution at the inlet and at the outlet of the apparatus for the two magnetization directions. Clearly, for a given magnetic direction one enantiomer is adsorbed on the Au. The opposite enantiomer is therefore in excess in the solution and dominates its CD spectrum. The results here indicate once again that the L enantiomer favors a surface that is magnetized up (i.e. H+), whereas the D enantiomer favors the down magnetization (i.e. H-).

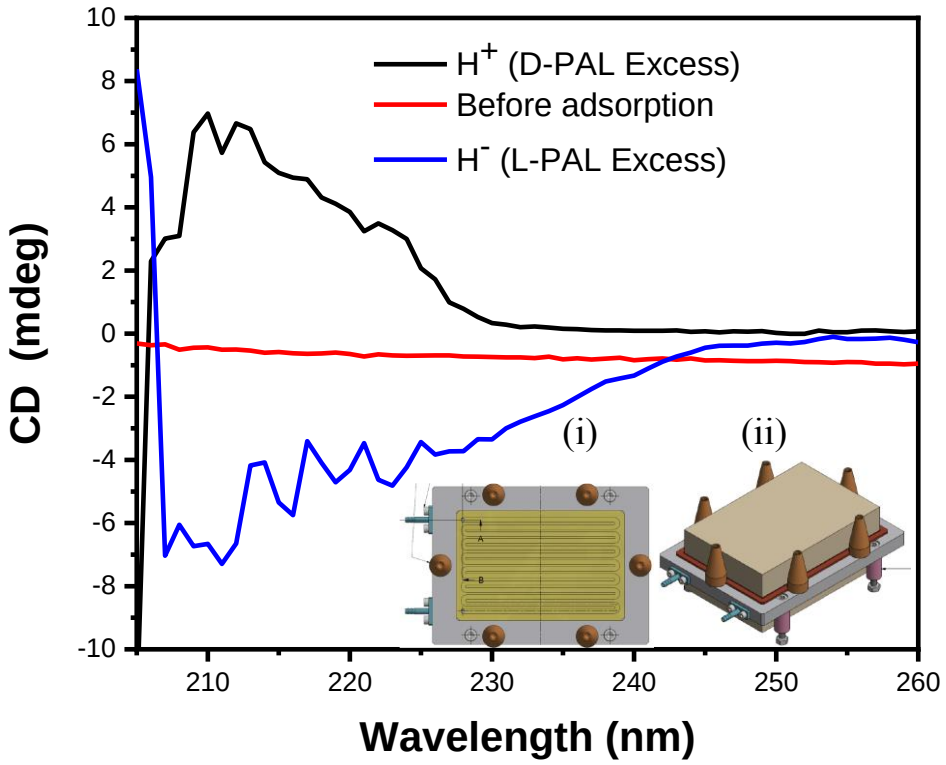

Figure 3: CD spectra of a racemic PAL mixture at the inlet (red) and at the outlet of a magnetic column (*i*), with an external (*ii*) magnetic field pointing up (black) or down (blue). Enantio-separation is clearly obtained.

To establish that the effect is not molecule-specific, we probed the enantio-selective effect for a small amino acid, cysteine. Briefly, solutions of L- or D-cysteine were exposed to magnetic substrates with the magnetization pointing up or down. To explore the kinetics of the process, the change in concentration was measured by applying high-performance liquid chromatography (HPLC). We define the adsorption specificity as $\frac{A_D - A_U}{A_D + A_U}$, where A_D and A_U denote the amount of adsorbed molecules measured for the two magnetization directions, namely, up or down, respectively. The results, presented in Figure 4, indicate that for short adsorption times the adsorption is enantio-selective exactly as before. For long adsorption times the selectivity is lost, a result which is again consistent with that obtained for PAL and indicating different adsorption rates on the magnetized substrate.

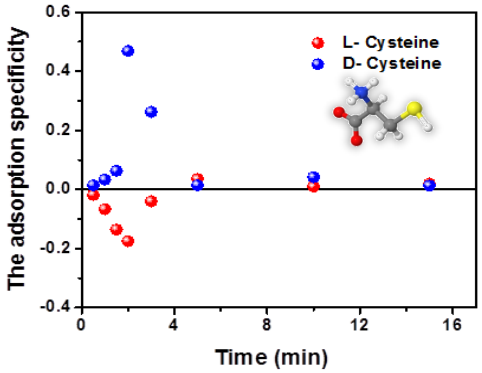

Figure 4: Adsorption specificity, defined as $\frac{A_D - A_U}{A_D + A_U}$, where A_D and A_U are HPLC-measured amounts of adsorbed molecules measured for adsorption on a magnetic substrate with magnetic moment pointing down or up, respectively, as a function of time, for solutions of L- and D-cysteine.

To monitor the kinetics of enantio-selective adsorption directly we used fluorescence measurements, where the signal is proportional to the number of adsorbed molecules. This was achieved by examining double-stranded DNA (dsDNA) molecules, to which a fluorescent dye was attached, thereby also facilitating a study of yet another chiral system. To that end, Cy-3 (cyanine) dye was tagged at the 3' position (cytosine) of the dsDNA (20 bp). The linker Cy-3 modifies the phosphate of cytosine (purchased from Integrated DNA Technology (IDT)). The dsDNA sequence that was used is given in the SI. In this case the molecules were adsorbed on a Ni/Au surface and the fluorescence was measured for different adsorption times and for different Ni magnetization directions (Figure 5a). Fig. 5b shows the adsorption as a function of time and demonstrates that the adsorption rate is significantly different for up and down magnetization of the substrate.

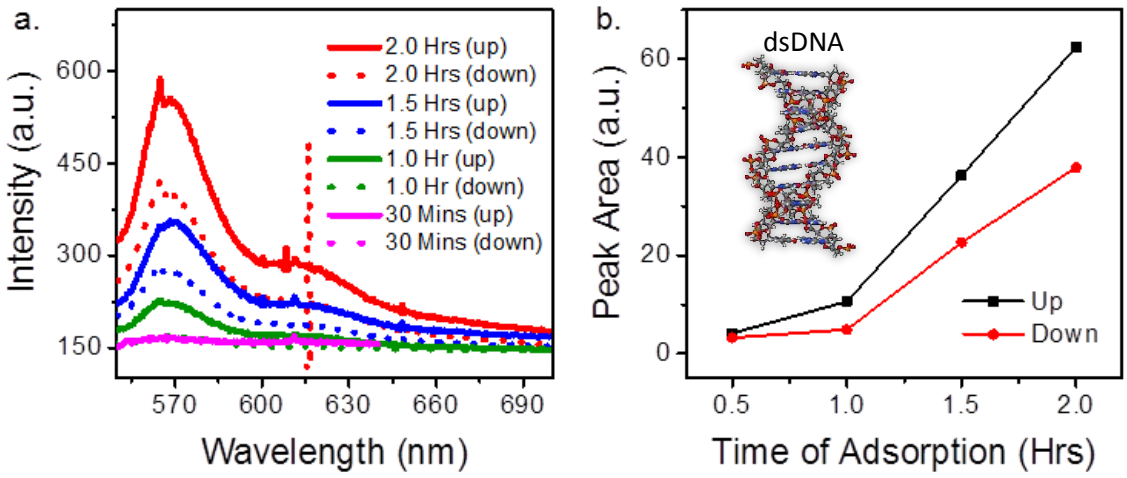

Figure 5: (a) Fluorescence spectrum measured from adsorbed dsDNA on a 7 nm Ni layer coated by an 8 nm thick gold layer, with the magnet pointing up or down. The vertical dashed line marks the border of the peak area. (b) Time dependence of the adsorption process obtained when the magnetic dipole of the substrate is pointing up (black) or down (red).

The above results demonstrate the generic nature of the effect. Unambiguous enantio-selectivity, based on different adsorption rates on a perpendicularly-magnetized FM substrate, is obtained throughout for a variety of chiral molecules. We now explain in more detail how this can be rationalized in terms of CISS-induced spin-polarization in the chiral molecule, facilitating a selective magnetic-exchange interaction with the FM substrate. Under electric dipole polarization, induced by the substrate, an excess of electrons and holes on the negative and positive pole of the molecule, respectively, is obtained. This charge polarization is accompanied by spin polarization, as previously shown both experimentally and theoretically (19,26). The specific spin orientation at each pole depends on the chirality of the molecule (see Fig. 6a). Importantly, the spin-polarization results from the *dynamic* process of the electron redistribution in the chiral potential presented by the molecule.

If there is an exchange interaction between the molecular spin and the spin of the FM substrate, then the substrate-molecule interaction will be stabilized if the two spins are anti-parallel (low-spin configuration) and destabilized if they are parallel (high-spin configuration), as shown in Fig. 6b. Indeed, a prior study found that adsorption of chiral

molecules on a non-magnetized FM substrate tends to magnetize it in opposite directions for opposite enantiomers.(27)

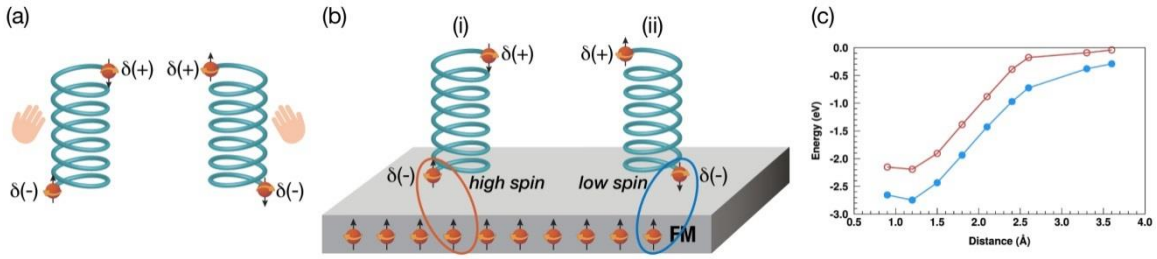

Figure 6: a. A scheme of the process occurring when a chiral molecule is polarized. The electrical polarization of the molecule is accompanied by spin polarization. The spin alignment at each electric pole depends on the specific enantiomer. b. Therefore, for a specific enantiomer the interaction between the magnetized surface and the molecule follows either a high spin (i) or a low spin (ii) potential, depending on the direction of magnetization of the substrate. c. Calculated interaction energies as a function of distance between a hydrogen atom and a surface represented by a 2x2x2 cube of Ni atoms. All spins of the Ni atoms aligned parallel to each other and the hydrogen atom spin aligned either parallel (red curve) or anti-parallel (blue curve) to the spin of the nickel atoms. At longer distances the two different configurations merge in terms of total energy and that energy is considered as the zero of the energy axis.

The remaining question, then, is whether this spin interaction is large enough to promote enantio-selectivity. To test that, we assume that spin-polarization has already been obtained through the dynamic CISS effect and study spin-interaction with the FM substrate. The simplest model possible for net spin-polarization is given by a hydrogen atom with a spin-polarized electron. We then represent the FM layer by a cube of nickel atoms with two atoms in each dimension, whose H-facing surface is oriented, along the (111) direction of bulk Ni, with spins aligned parallel to each other due to the ferromagnetic interaction. We performed density functional theory (DFT) exploring the interaction energies as a function of distance, using the Perdew-Burke-Ernzerhof (PBE) functional (28) (computational details are given in the SI). In one case, the H atom spin was considered to be along the same direction of all the Ni atoms (high spin, ferromagnetic configuration) and in the other in the opposite direction (low spin, anti-ferromagnetic configuration). Clearly, this is but a crude model for the real system, whose accuracy is further limited by known limitations on charge (29) and spin (30)

dissociation with conventional DFT. Nevertheless, the results, given in Fig. 6c, show that for all the distances up to about 0.35 nm, the total energy of the system for the high spin configuration is higher than that of the low spin configuration. The energy difference at the minimum of the potential is of the order of 0.6 eV, which is well above thermal energy at room-temperature. The hydrogen atom represents an extreme case of charge polarization (a full electron). However, even if only one tenth of an electron charge is polarized, the difference between the two spin states would still easily allow for an observable effect.

To show that a similar effect is obtained with a more realistic molecular model, we considered a small chiral molecule, $CH_3C(OH)H(NH)$, whose radical character results in a net spin-polarization in the gas-phase. Interaction energy curves, similar to those shown in Figure 6c, are given in Fig. S3 of the SI. Here too, the energy difference is sizeable (~0.4 eV at the minimum of the potential) and decaying with increasing molecule-substrate separation, despite the spin on the atoms close to the surface being less than that of a full electron.

The curves of Fig. 6c show two binding potential landscapes. If the molecule-surface interaction time is long enough, the molecular spin-orientation may flip, due to spin-orbit coupling or hyperfine interactions, and the molecule will interact with the surface on the lower potential energy surface (see also (31) for a discussion in terms of "true" and "false" chirality). However, at short times, each spin-polarization will experience a different interaction potential and therefore different adsorption kinetics, consistent with the experimental results of Figs. 4 and 5b.

We emphasize once again that the effect reported here is not associated with the *direct* interaction of chiral molecules with magnetic fields,(32-35) but rather with the magnetic-exchange interaction of the spin-polarized molecules with the spin-polarized substrate (See Figs. 1e, 6b). The direct interaction energy of an electron spin with a magnetic field is typically of the order of μeV, while the interaction energies obtained in Fig. 6c are at least five orders of magnitude larger.

Enantio-separation is an extremely important process in the pharmaceutical and chemical industries. Chromatography and electromigration techniques have long been the methods of choice in this field.(36-45) However, despite intensive efforts, obtaining

enantiomerically pure synthetic materials remains a challenge, as the cost of separation is relatively high and an extensive effort is required. The enantio-selective interaction of chiral molecules with a magnetic substrate provides a generic chromatographic method for enantio-separation, which does not require a specific separating column. Because the observed effect depends on the electrical polarizability of the system (that is accompanied by spin polarization) and because this polarization depends on the global structure of the chiral molecule, the method described here may also allow the separation of chiral molecules from a mixture of molecules, either chiral or achiral. In addition, this technique may be applied for separating chiral molecules based on their secondary structure and/or for separating two secondary structures of the same chiral molecule.

In summary, we have presented results that prove significant enantio-selectivity based on the adsorption rate of chiral molecules on magnetic substrates, opening up the possibility of separating enantiomers by a generic column that does not have to be modified when separating different molecules.

Acknowledgements

We thank Dr. Alexander Brandis for performing the HPLC measurements. YP and RN acknowledge the support of the John Templeton Foundation. RN acknowledges the supported by the Israel Science Foundation and by the European Research Council under the European Union's Seventh Framework Program (FP7/2007-2013)/ERC grant agreement n° 338720 CISS. YP acknowledges the support of the Israel Science Foundation and the Ministry of Science Israel. OBD acknowledges the support from the Israeli Ministry of Science, Technology and Space grant # 0399174.

Author contributions.

KB-G performed the experiments on the DNA and with the HPLC, OBD performed the adsorption experiments on the oligopeptides, FT performed the experiments applying the CD, EC prepared the setup for the adsorption experiments, SY prepared and characterized the oligopeptides, AC S-HY and SSPP designed, prepared and characterized the Ni substrates, SS performed and analyzed the calculations, LK participated in planning and analyzing the calculations and in writing the manuscript, LTB designed, prepared and characterized the Co surfaces, RN and YP conceived the experiments and LK, YP, and RN wrote the manuscript.

References

[1] L. D. Barron, *Chem. Soc. Rev.*,**15**, 189-223 (1986).

[2] T. Ruchon, M. Vallet, J.-Y. Thépot, A. Le Floch, R. W. Boyd, *C. R. Physique* **5,** 273–277 (2004).

[3] L. Pasteur, *Rev. Scient.* 3, vii : 2-6, Oeuvres I : 369 (1884).

[4] S.F. Mason, *Nature* **311,** 19-23 (1984).

[5] P. Frank, W.A. Bonner, R.N. Zare, in: E. Keinan, I. Schechter (Eds.), Chemistry for the 21st Century, Wiley, 2001.

[6] K. Okano, O. Arteaga, J. M. Ribo, T. Yamashita, *Chem. Eur. J.*, **17**, 9288 – 9292 (2011).

[7] K. Okano, T, Yamashita, *ChemPhysChem*, **13**, 2263 – 2271 (2012).

[8] B.L. Feringa, R. A. Van Delden, *Angew. Chem. Int. Ed.* **38,** 3418- 3438 (1999).

[9] Lord Kelvin, Baltimore Lectures, Clay, London, 1904.

[10] P. Curie, *J. Phys.* **3,** 393-415 (1894).

[11] P.-G. De Gennes, *C. R. Acad. Sci. Paris, Sér. B* **270** 891 (1970).

[12] R. Naaman, D. H. Waldeck, *Ann. Rev. Phys. Chem*. **66**, 263–81 (2015).

[13] K. Michaeli et al., *Chem. Soc. Rev.* **45,** 6478 (2016).

[14] T. J. Zwang, S. Hürlimann, M. G. Hill, J. K. Barton, *J. Am. Chem. Soc.*, **138**, 15551–15554 (2016).

[15] R. A. Rosenberg, D. Mishra, R. Naaman, *Angew. Chemie*, **54**, 7295-7298 (2015).

[16] A. C. Aragonès et al. *Small* **13**, 1602519 (2017).

[17] M. Kettner, D. K. Bhowmick, M. Bartsch, B. Göhler, H. Zacharias, *Adv. Mater. Interfaces*, **3**, 1600595 (2016).

[18] J. M. Abendroth et al. *ACS Nano* **11**, 7516–7526 (2017).

[19] A. Kumar et al., *Proc. Nat. Acad. Sc.* **114** , 2474–2478 (2017).

[20] L. D. Barron, *Nature* **405**, 895-896 (2000).

[21] D. E. Koshland, *Angew. Chem. Int. Ed.*, **33**, 2375–2378 (1994).

[22] Y. Zhang, D.-R. Wu, D. B. Wang-Iverson, A. A. Tymia, *Drug Discovery Today*, **10**, 571-577 (2005).

[23] M. Johnson, *J. App. Phys.* **75,** 6714-6719 (1994).

[24] Handbook of Spin Transport and Magnetism, ed. E. Y. Tsymbal, I. Zutic, CRC Press (2012).

[25] M. Johnson, *Science* **260**, 320-323 (1993).

[26] K. Michaeli et al. *J. Physics: Condensed Matter*, **29**, 103002 (2017)

[27] O. Ben Dor et al., *Nat. Comm*. **8**,14567 (2017).

[28] J. P. Perdew, K. Burke, M. Ernzerhof, *Phys. Rev. Lett*. **77,** 3865 (1996).

[29] J.P. Perdew, R. G. Parr, M. Levy, J. L. Balduz, *Phys. Rev. Lett.* **49**, 1691 (1982).

[30] J.P. Perdew, A. Savin, K. Burke, *Phys. Rev. A* **51**, 4531 (1995).

[31] L.D. Barron, *Chirality*, **24**, 957– 958 (2012).

[32] H. J. Choi, M. H. Hyun, *Chem. Commun.*, **42**, 6454−6456 (2009).

[33] S. G. Kozlova, M. R. Ryzhikov, N. B. Kompankov, M. S. Zavakhina, *J. Phys. Chem. B*, **120**, 7517−7521 (2016).

[34] N. Micali, H. Engelkamp, P. G. van Rhee, P. C. M. Christianen, L. Monsù Scolaro, J. C. Maan, *Nat. Chem.*, **4,** 201−207 (2012).

[35] L.D. Barron, Science, 266,1491-1492 (1994).

[36] J. Itoh, K. Fuchibe, T. Akiyama, *Angew. Chem., Int. Ed.*, **45**, 4796−4798 (2006).

[37] K. Gedrich, I. Senkovska, I. A, Baburin, U. Mueller, O.Trapp, S. Kaskel, *Inorg. Chem.*, 49, 4440−4446 (2010).

[38] R. Vaidhyanathan, D. Bradshaw, J. N. Rebilly, J. P. Barrio, J. A. Gould, N. G. Berry, M. J. Rosseinsky, *Angew. Chem., Int. Ed.*, **45**, 6495−6499 (2006).

[39] A. V. Davis, D. Fiedler, M. Ziegler, A. Terpin, K. N. Raymond, *J. Am. Chem. Soc.*, **129**, 15354−15363 (2007).

[40] T. Liu, Y. Liu, W. Xuan, Y. Cui, *Angew. Chem., Int. Ed.* 49, 4121−4124 (2010).

[41] S. Inagaki, J. Z. Min, T. Toyo'oka, *Anal. Chem.*, **80**, 1824−1828 (2008).

[42] B. S. Sekhon, *Int. J. Chem Tech Res.*, **2**, 1584−1594 (2010).

[43] S. C. Ng, L. Chen, L. F. Zhang, C. B. Ching, *Tetrahedron Lett.*, **43**, 2863−2866 (2002).

[44] Y. Zhang, D. R. Wu, D. B. Wang-Iverson, A. A. Tymiak, *Drug Discovery Today*, **10**, 571−577 (2005).

[45] G. Gübitz, M.G. Schmid, *Electrophoresis*, **23**, 3981-96 (2004).

Supplementary Information

Separation of Enantiomers by Enantio-Specific Interaction of Chiral Molecules with Magnetic Substrates

Koyel Banerjee-Ghosh,[1$] Oren Ben Dor,[2$] Francesco Tassinari,[1$] Eyal Capua,[1] Shira Yochelis,[2] Amir Capua,[2] See-Hun Yang,[3] Stuart Stephen Papworth Parkin,[3,4] Soumyajit Sarkar,[5] Leeor Kronik,[5] Lech Tomasz Baczewski,[6] Ron Naaman,[1*] and Yossi Paltiel[2*]

1) Dept. of Chemical and Biological Physics, Weizmann Institute of Science, Rehovot, 76100 Israel
2) Dept. of Applied Physics, Hebrew University, Jerusalem, Israel
3) IBM Research Division, Almaden Research Center, 650 Harry Road, San Jose, California 95120, USA
4) Max Planck Institute for Microstructure Physics, Halle (Saale), D-06120, Germany
5) Department of Materials and Interfaces, Weizmann Institute of Science, Rehovot, 76100 Israel
6) Institute of Physics Polish Academy of Sciences, Al. Lotnikow 32/46, 02-668 Warszawa, Poland.

PAL adsorption measurements

During the adsorption measurements we used a fixed concentration of 1 mM of PAL molecules in ethanolic solution. Both D-PAL (Fig. S1) and L-PAL (Fig. S2) molecules were adsorbed by SAM method on a superparamagnetic (SPM) substrate (100 Al_2O_3 | 20 TaN | 30 Pt | 1.5 Co | 20 Au, units in Å), while placed under an external magnetic field of ±3000 G at room temperature (RT) and under inert conditions. The magnetic field was

applied perpendicular to the surface facing up (+) or down (-). Different adsorption durations were tested for both magnetic orientations: <1 sec, 2 sec, 10 sec, 20 sec, 30 sec, 1 min, 2 min and 10 min. Immediately after adsorption, samples were rinsed in absolute ethanol, without applying a magnetic field, in order to remove un-adsorbed molecular residues, and then dried by nitrogen.

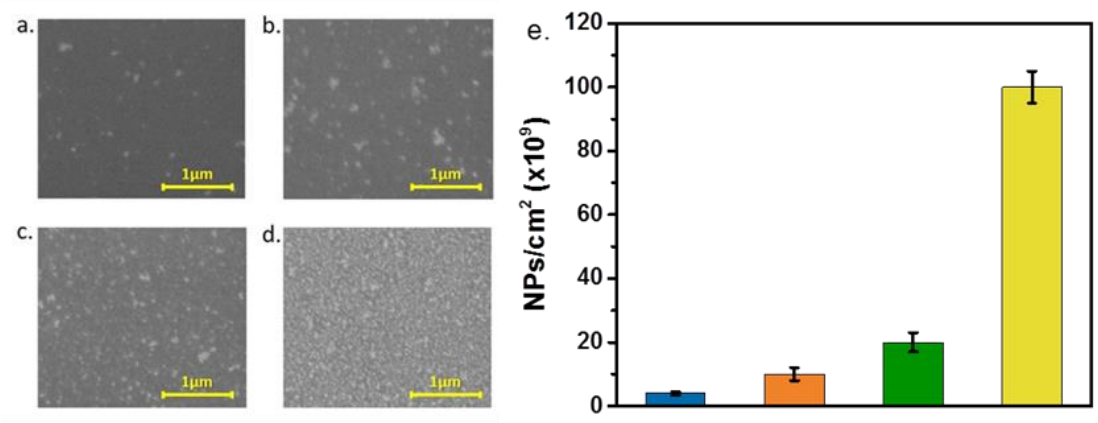

Figure S1. Time dependent adsorption of D-PAL molecules. Different superparamagnetic samples were immersed in a 1 mL ethanolic solution of 1 mM D-PAL during 1 sec while a +3000 G magnetic field is applied, yielding a concentration of ~$4 \cdot 10^9$ NPs/cm^2, whereas a -3000 G perpendicular magnetic field yields a concentration of ~$1 \cdot 10^{10}$ NPs/cm^2 (a and b, respectively). This process was repeated for a 10 min adsorption duration as a +3000 G applied magnetic field yields a concentration of ~$2 \cdot 10^{10}$ NPs/cm^2, and a -3000 G perpendicular magnetic field results in a concentration of

~$1 \cdot 10^{11}$ NPs/cm^2 (c and d, respectively). All samples were immersed in a solution of 0.15 %wt SiO_2 NPs in water for 2 min and then dried. e. Histograms depicting D-PAL adsorptions under +3000 G (blue) and -3000 G (orange) during 1 sec and adsorptions under +3000 G (green) and -3000 G (yellow) during 10 min.

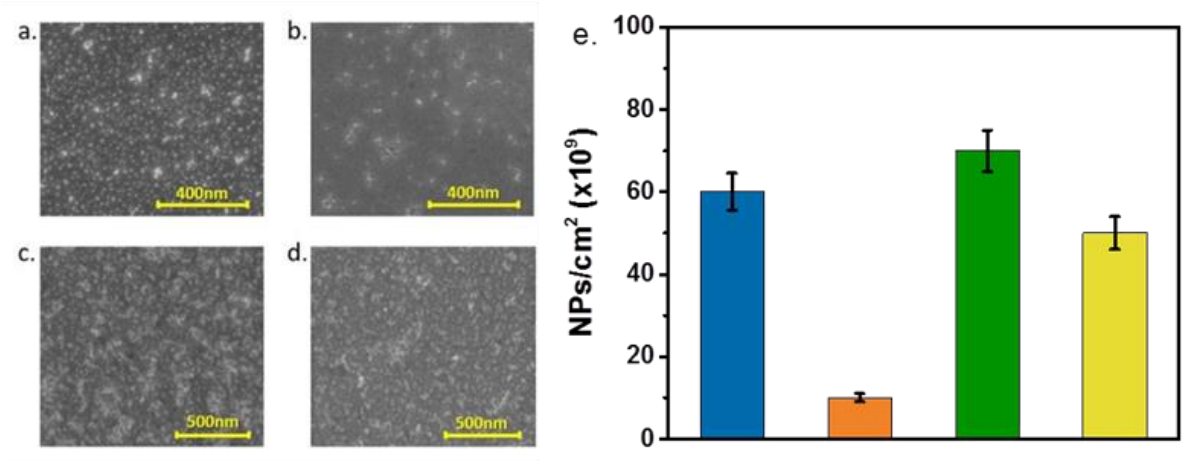

Figure S2: Time dependent adsorption of L-PAL molecules. Different superparamagnetic samples were immersed in a 1 mL ethanolic solution of 1 mM L-PAL during <1 sec while a +3000 G perpendicular magnetic field yields a concentration of

~$6 \cdot 10^{10}$ NPs/cm^2, and a -3000 G perpendicular magnetic field yields a concentration of ~$1 \cdot 10^{10}$ NPs/cm^2 (a and b, respectively). This process was repeated for a 2 min adsorption duration as a +3000 G perpendicular magnetic field yields a concentration of ~$7 \cdot 10^{10}$ NPs/cm^2 and a -3000 G perpendicular magnetic field yields a concentration of ~$5 \cdot 10^{10}$ NPs/cm^2 (c and d, respectively). All samples were immersed in a solution of 0.15% wt SiO_2 NPs in water for 2 min and then dried. e. Histograms depicting L-PAL adsorption under +3000 G (blue) and -3000 G (orange) during <1 sec and adsorptions under +3000 G (green) and -3000 G (yellow) during 2 min.

Similar time-dependent adsorptions were conducted on molecular beam epitaxy (MBE) grown epitaxial FM thin film magnetic samples with perpendicular anisotropy (Al_20_3 (0001) | Pt 50 | Au 200 | Co 18 | Au 50, units in Å), as can be seen in Fig. S2. The FM samples were magnetized by an external magnetic field of ±3000 G at RT and under inert conditions. The coercive field of the FM samples used was ~215 G. The FM samples' easy axis was out-of-plane (OOP) thus ensuring that the applied magnetic field would reorient the magnetization OOP parallel or anti-parallel to surface normal.
All samples were then immersed in a solution of 0.15 wt% SiO_2 amorphous nanocrystals (NCs) in H_2O (mkNANO), without any magnetic influence, for 2 min, and then rinsed in H_2O. The NCs were used in order to mark the adsorbed molecules location on the substrate.

DNA adsorption experiment

The DNA double stranded solutions for the SAM incubation were prepared using a functionalized double stranded DNA (purchased from Integrated DNA Technologies), having the following structure:

5' GAC CAC AGA TTC AAA CAT GC - *Thiol-Modifier-C3 S-S* **3'**

3' *Cy3* – CTG GTG TCT AAG TTT GTA CG **5'**

A 100 μM stock solution was prepared using deionized water as the solvent. The solutions for the SAM preparation were prepared by mixing 100 μL of the stock solution

and adding 100 μL of a phosphate buffer 0.8 M (pH 7.2), to obtain 200 μL of a 50 μM DNA solution in 0.4 M phosphate buffer (pH 7.2). This solution underwent a thermal incubation (10 minutes at 90 °C, then cooled down to 15 °C at a ramp of 1 °C every 45 sec) to anneal the DNA strands into a double stranded DNA. After this, 200 μL of a 10 mM Tris(2-carboxyethyl)phosphine hydrochloride (purchased from Sigma Aldrich) in 0.4 M buffer phosphate (pH 7.2) were added to the DNA solution to remove the thiol-protecting group, and the resulting solution was left to react for 2 h. The product was purified by filtering the solution with a Micro Bio-Spin P-30 column (purchased from Bio Rad). The final concentration of the DNA solution was finally checked by UV-vis spectroscopy using a Nanodrop spectrometer, resulting in a 22 mM DNA concentration.

The adsorption experiments were performed using 1x1 cm^2 FM samples (Si <100> | 80 Ti | 1000 Ni | 80 Au, units in Å). The surfaces were cleaned by boiling in acetone and in ethanol for 10 min each, followed by a UV/OX treatment for 10 min, and then immersing in ethanol for 30 min.

Immediately after drying them with a nitrogen flow, the surfaces were placed in a magnetic field of 3000 G, directed away (+) or into (-) the surfaces. Different adsorption durations were tested for both magnetic orientations: <30 min, 1 h, 1.5 h, >2 h. Immediately after adsorption, samples were rinsed twice in phosphate buffer 0.4 M (pH 7.2) and twice in DI water, without applying a magnetic field, in order to remove unwanted molecular residues, and then dried by nitrogen.

The fluorescence of the monolayers was measured using a LabRam HR800-PL spectrofluorimeter microscope (Horiba Jobin-Yivon). For the excitation of the dye, a 532 nm laser light (DJ532-40 laser diode, ThorLabs, at a power of ~1.65 mW/cm^2) was used. The spectra were collected using a microscope (with a ×10 high-working distance lens) from 9 different points (mapping from 3x3 matrix) and then averaged out. During the measurement, a confocal aperture (1100 μm) was fully opened, and the integration time was maintained at 15 sec.

Cysteine adsorption experiment

A 1 mL volume of a 1 μM solution of either L- or D-cysteine was prepared by dissolving the amino-acid in a 10 mM citrate buffer solution (pH 3). The solution was purged with argon for 5 minutes before use. A 1x1 cm^2 FM sample (Si <100> | 80 Ti | 1000 Ni | 80 Au, units in Å) was dipped into the solution under a magnetic field of 3000 G, directed away (+) or into (-) the surface. Different adsorption durations were tested for both magnetic orientations: 0 sec, 30 sec, 1 min, 1.5 min, 2 min, 5 min, 10 min, and >15 min. After adsorption, the concentration of the amino-acid left in the solution was measured by HPLC-MS. HPLC-MS measurements were done by derivatizing the cysteine column prior to injection by adding to a 10 μL of sample solution a mixture of 70 μL of AccQ•Tag™ Ultra Borate Buffer and 20 μL of AccQ•Tag™ Ultra reagent (6-aminoquinolyl-N-hydroxysuccinimidyl carbamate; AQC) both purchased by Waters, followed by incubation for 30 min at 55°C. Following this incubation, a 1 μL of the dye-functionalized cysteine solution were injected to the HPLC-MS equipped with a Waters AccQ-Tag Ultra column (2.1 mm i.d. × 100 mm, 1.7 μM particles). The separation was carried on with a linear gradient (from A=99.9% to A=40% in 10 min) and a flow rate of 0.7 mL/min. The working eluent A was a mixture of acetonitrile (10%), formic acid (6%), and ammonium formate in water (84%); while eluent B was 100% acetonitrile. To quantify the concentration, the intensity of the 171.01 m/z diagnostic ion, corresponding to the fragmentation of the AQC dye, was considered. The difference between the concentration found for time equal 0 sec and the concentration found at the various adsorption times was considered to be directly proportional to the amino acid adsorbed on the surfaces.

Multiple adsorption of a racemic PAL mixture

Our initial racemic mixture consisted of 1 μM of D-PAL and 1 μM of L-PAL in an ethanolic solution. We rinsed a 4×4 mm^2 SPM sample in the racemic solution under the influence of a +3000 G external magnetic field for ~1 sec. We transferred 1 ml from the remaining solution into a cuvette. We then adsorbed 99 additional 4×4 mm^2 SPM samples in the same way. After 100 samples' adsorptions, we extracted an additional 1

ml from the remaining solution and placed it in a cuvette. The same procedure was repeated with a new racemic mixture for a -3000 G external magnetic field.

The CD measurements were carried out using a Chirascan spectrometer, Applied Photo Physics, England. The measurement conditions for all spectra were done at a scan range of 210 to 400 nm; 2 sec time per point; 1 nm step size; and a 1 nm bandwidth. The quartz cuvette used had an optical pathway of 1 cm.

The L- and D-PAL enantio-pure solutions were prepared by diluting 3 mg of the oligopeptide (purchased from Sigma-Aldrich and used as received) in 1 mL of ethanol, obtaining a 1 mM solution of both. The CD of these enantio-pure 1 µM solutions is reported in the main manuscript (Fig. 2B). In order to produce a racemic mixture, two aliquots of the above stock solutions were mixed together to a 1:1 ratio.

The CD spectra reported in the main manuscript (Fig. 2A) is the difference between the CD spectra of the racemic mixture after the first adsorption (used as the baseline) and the CD spectra of the same solution after 100 adsorptions, for each of the two magnetic fields. The data was smoothed and the relative standard deviation is reported in the graph as the lighter area around the curves.

Calculations

All calculations were carried out using density functional theory (DFT) within the generalized-gradient approximation (GGA), using the Perdew-Burke-Ernzerhof (PBE) functional. Calculations of H atom-Ni surface interaction were performed using the cc-pVTZ basis set, as implemented in the Gaussian 2009 (G09) code [1]. Calculations of the small chiral molecule, $CH_3C(OH)H(NH)$, interaction with the Ni surface were performed using the plane-wave basis set based VASP code,[2] in which ion-electron interactions are treated with the projector augmented wave (PAW) approach.[3,4]. For the chiral molecule, calculations were augmented by dispersive interactions of the type described in Ref. [5].

A 2x2x2 “cube” of Ni, set along (111) direction of the face centered cubic (FCC) unit-cell of bulk Ni, was theoretically optimized until the force components of every Ni atom was less than 0.002 eV/Å. In addition, the chiral molecule was theoretically optimized

until the force components of each atom was below 0.001 eV/Å. A single H atom/chiral molecule was placed at a height *z* above the plane of the top layer of the Ni cube. The distance of the H atom/chiral molecule from the Ni plane was varied over a range. For each distance, two different spin configurations were considered. In one case, the spin on H atom/chiral molecule was considered to be along the same direction of that of all the Ni atoms (high spin, ferromagnetic configuration) and in the other, the spin on H atom/chiral molecule was considered along the opposite direction (low spin, anti-ferromagnetic configuration). A Mulliken charge analysis of the converged electronic structure was used to verify the expected relative orientation of the spin on the H atom/chiral molecule with respect to the Ni spins, for each individual calculation. In the case of H atom-Ni surface calculations, self-consistency of electronic density was such that the difference of total energy between two consecutive iterations was below 10^{-5} eV. Further reduction was not possible owing to numerical fluctuations.

The chiral molecule-Ni surface calculations were carried out imposing a constraint on the total spin magnetic moment of the overall system in order to obtain the high spin (molecule spin remains parallel to the Ni spins) or low spin (molecule spin aligns opposite to the Ni spins) configuration. Our calculations, summarized in Figure 6C of the main text and Fig. S3 below, show that the total energy of the system for the low spin (LS) configuration is lower than that of the high spin (HS) configuration.

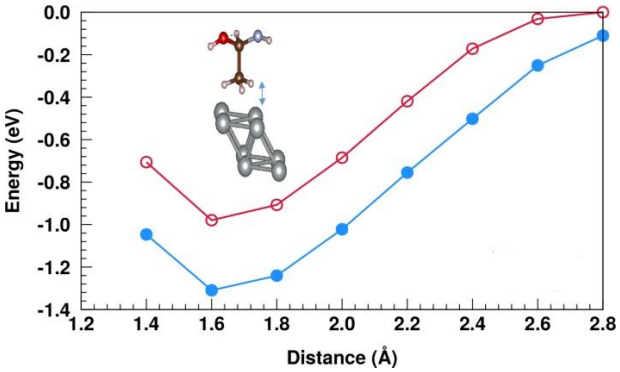

Figure S3: Calculated interaction energies as a function of distance between a chiral molecule and a surface represented by a 2x2x2 cube of Ni atoms. All spins of the Ni atoms are aligned parallel to each other and the molecular spin is initially either parallel (red empty circle curve) or anti-parallel (blue filled circle curve) to the spin of the nickel

atoms. At large distances, the two different configurations merge in terms of total energy and this energy is considered as the zero of the energy axis. The Inset shows the geometry of the chiral molecule and the Ni surface at a typical separation, indicated by the arrow.

References:

[1] Gaussian 09, Frisch, M. J.; Trucks, G. W.; Schlegel, H. B.; Scuseria, G. E.; Robb, M. A.; Cheeseman, J. R.; Scalmani, G.; Barone, V.; Mennucci, B.; Petersson, G. A.; Nakatsuji, H.; Caricato, M.; Li, X.; Hratchian, H. P.; Izmaylov, A. F.; Bloino, J.; Zheng, G.; Sonnenberg, J. L.; Hada, M.; Ehara, M.; Toyota, K.; Fukuda, R.; Hasegawa, J.; Ishida, M.; Nakajima, T.; Honda, Y.; Kitao, O.; Nakai, H.; Vreven, T.; Montgomery, J. A., Jr.; Peralta, J. E.; Ogliaro, F.; Bearpark, M.; Heyd, J. J.; Brothers, E.; Kudin, K. N.; Staroverov, V. N.; Kobayashi, R.; Normand, J.; Raghavachari, K.; Rendell, A.; Burant, J. C.; Iyengar, S. S.; Tomasi, J.; Cossi, M.; Rega, N.; Millam, J. M.; Klene, M.; Knox, J. E.; Cross, J. B.; Bakken, V.; Adamo, C.; Jaramillo, J.; Gomperts, R.; Stratmann, R. E.; Yazyev, O.; Austin, A. J.; Cammi, R.; Pomelli, C.; Ochterski, J. W.; Martin, R. L.; Morokuma, K.; Zakrzewski, V. G.; Voth, G. A.; Salvador, P.; Dannenberg, J. J.; Dapprich, S.; Daniels, A. D.; Farkas, Ö.; Foresman, J. B.; Ortiz, J. V.; Cioslowski, J.; Fox, D. J. Gaussian, Inc., Wallingford CT, 2009.

[2] G. Kresse, J. Furthmüller, *Phys. Rev. B* **54**, 11169 (1996).

[3] P. E. Blöchl, *Phys. Rev. B* **50**, 17953 (1994).

[4] G. Kresse, D. Joubert, *Phys. Rev. B* **59**, 1758 (1999).

[5] V. G. Ruiz, W. Liu, E. Zojer, m. Scheffler, and A. Tkatchenko, *Phys. Rev. Lett.* **108**, 146103 (2012).